Friction of atomically stepped surfaces

Dikken, R. J.; Thijsse, B. J.; Nicola, L.

DOI
10.1103/PhysRevB.95.104106

Publication date
2017

Document Version
Final published version

Published in
Physical Review B (Condensed Matter and Materials Physics)

Friction of atomically stepped surfaces

R. J. Dikken,* B. J. Thijsse, and L. Nicola
Department of Materials Science and Engineering, Delft University of Technology, 2628CD Delft, the Netherlands
(Received 7 November 2016; published 20 March 2017)

The friction behavior of atomically stepped metal surfaces under contact loading is studied using molecular dynamics simulations. While real rough metal surfaces involve roughness at multiple length scales, the focus of this paper is on understanding friction of the smallest scale of roughness: atomic steps. To this end, periodic stepped Al surfaces with different step geometry are brought into contact and sheared at room temperature. Contact stress that continuously tries to build up during loading, is released with fluctuating stress drops during sliding, according to the typical stick-slip behavior. Stress release occurs not only through local slip, but also by means of step motion. The steps move along the contact, concurrently resulting in normal migration of the contact. The direction of migration depends on the sign of the step, i.e., its orientation with respect to the shearing direction. If the steps are of equal sign, there is a net migration of the entire contact accompanied by significant vacancy generation at room temperature. The stick-slip behavior of the stepped contacts is found to have all the characteristic of a self-organized critical state, with statistics dictated by step density. For the studied step geometries, frictional sliding is found to involve significant atomic rearrangement through which the contact roughness is drastically changed. This leads for certain step configurations to a marked transition from jerky sliding motion to smooth sliding, making the final friction stress approximately similar to that of a flat contact.

DOI: 10.1103/PhysRevB.95.104106

I. INTRODUCTION

Friction of rough surfaces is the outcome of multiple asperities of different size being flattened and sheared. However, even contacts at the nanoscale can exhibit roughness in the form of atomic scale steps. Such steps are essentially the smallest scale of roughness and can originate, for example, from crystal growth [1,2] or the escape of dislocations through surfaces [3–5] and are known to affect friction [6]. Several experimental studies [7–9] have revealed that the friction stress of a tip dragged along a stepped surface is larger compared to the friction stress of a tip dragged on an atomically flat surface. The reason for this increase has been attributed to the surface potential landscape [7,9] associated to stepped surfaces, where an additional barrier to motion, the Ehrlich-Schwoebel barrier [10,11], has to be overcome in the direction perpendicular to the step. Consistently with these findings, interface imperfections, of the type of steps and ledges, have been found to increase the shear strength of various interfaces, as those of metallic multilayers [12]. Furthermore, it has been hypothesized that static friction increases due to defects like vacancies and impurities at the interface that allow surfaces to sink into their pinning potentials despite the elastic energy that this costs [13].

The aim of this study is to understand the role of atomic scale steps on the frictional behavior of metal contacts. The size of the steps considered here is in the order of the dislocation Burgers vector (up to 7b). We are interested in understanding whether these steps will maintain their size during contact sliding, or evolve towards a flatter surface, and through which atomic processes this would occur. Another question we intend to answer is whether the stress concentration associated with the step is sufficient to nucleate dislocations under moderate contact loading, and how dislocation nucleation would contribute to frictional sliding. Molecular dynamics simulations of the deformation of polycrystalline metals have shown a competition between stress relaxation by dislocation glide and by grain boundary slip [14]. Since in a molecular dynamics simulation grain boundaries and dry nanocontacts do not differ much, we are interested in verifying whether a similar competition between dislocation nucleation and slip can be found also for the stepped contacts. If dislocations were to play a role during frictional sliding of stepped contacts, their behavior would be markedly different than that of flat contacts.

Whether or not the frictional behavior of flat and stepped contacts is intrinsically different might have implications also in relation to the self-organized criticality of friction. In the past three decades, the concept of self-organized criticality has been introduced to explain physical processes involving dissipation [15,16]. In one of the first works on self-organized criticality (SOC), it has been hypothesized that this concept is underlying for spatial and temporal scaling in dissipative non-equilibrium systems [16]. This is certainly interesting in the context of friction, where the length scales involved differ by orders of magnitude. Several experimental and theoretical studies have confirmed the existence of SOC in sliding friction [17–20].

In this work, it is found that both flat and stepped surfaces present self-organized criticality. However, the atomic mechanisms that come into play are very different for stepped and flat contacts. Stress relaxation of flat contacts occurs purely by contact slip, while for stepped contacts the steps can move along the contact plane, resulting in normal contact migration. Although the mechanisms are different the power law statistics are affected rather minimally.

The paper is organized as follows. In Sec. II, the computational approach and problem formulation are presented. In Sec. III, the friction behavior of single step surfaces in contact is analyzed. In Sec. IV A, this is continued for step pair surfaces in contact. Section IV B is devoted to the study of step pair

*R.J.Dikken@tudelft.nl

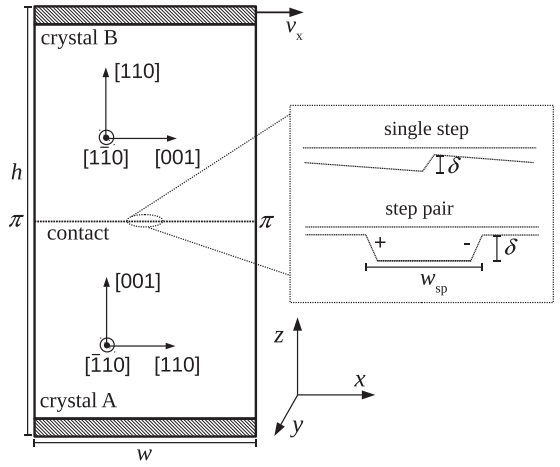

FIG. 1. Schematic representation of the model. The step height δ varies and relates to the lattice constant a, i.e., the Burgers vector $b = a/\sqrt{2}$.

surfaces of larger height, i.e., nanoscale asperities. Finally, the conclusions are presented in Sec. V.

II. COMPUTATIONAL APPROACH AND PROBLEM FORMULATION

The molecular dynamics (MD) simulations are performed using LAMMPS [21] with an EAM potential [22] developed by Purja Pun and Mishin [23–25]. This potential has shown to give accurate surface and stacking fault energies, making it especially suitable for studying the mechanical behavior of contacts and interfaces.

In this work, we focus on fcc metals. Aluminum has a large stacking fault energy, which entails that the separation of the two partials, by which a dislocation exists in an fcc metal, is small. This limits the necessary dimensions of the simulation box, and hence the simulation time. Some of the simulations were repeated with nickel and we could indeed verify that the results obtained in this study are qualitatively similar for different fcc metals. It is therefore expected that the qualitative results in general apply to ultraclean, oxide-free fcc metal surfaces. Although we are aware that aluminum has a high oxidation rate, and that such ultraclean, oxide-free metal surfaces are less realistic, this is convenient for the aim of this study, which is to fundamentally understand the effect of steps on friction.

The contact is formed between two crystals with the same height (in the z-direction, perpendicular to the contact plane) $h/2 = 45$ nm, so that the total height is $h = 90$ nm. The width w in the periodic x direction is varied between 15 and 45 nm. The periodic y direction is taken short, $d = 2$ nm, so that the steps are straight line-defects in the contact (see Fig. 1).

The two crystal orientations that are chosen both have symmetric slip systems for which the (dislocation) slip line lies along the short y-axis and are shown in Fig. 1.

Both periodic steps and step pairs (see Fig. 1) are studied. Periodic steps are created by applying vertical displacements to atoms in the lower crystal, such that at the periodic boundary the applied vertical displacement is zero and in the middle of the simulation cell it is δ (see Fig. 1). The periodic boundary

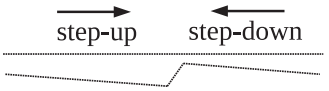

FIG. 2. Schematic representation of the two loading directions for periodic (single) step contacts.

conditions in the x direction effectively let us investigate a periodic array of steps. We here assume that the steps can emerge due to the absorption of impinging dislocations from the crystal. In Ref. [3], it is found that maximum two dislocations can be absorbed at the same impingement site. Therefore the height of the step δ (in the z direction) is taken to be $a/2$ or a, which represents 1 or 2 escaped dislocations, respectively.

The step pairs are created by removing atomic planes parallel to the crystal surfaces (see Fig. 1). This creates two steps of opposite sign.

The distance between the two crystals is initially a. The contact forms during a relaxation run. Depending on the step height, a closed contact or a contact with a gap (free surfaces) forms. In this work, a vertical atomic separation smaller than one lattice parameter a is defined as a "closed" contact, otherwise as a gap.

After the system is relaxed, ten atomic planes at the top of the upper crystal are displaced in the x direction over a distance of 40 nm with a constant velocity $v_T = 2$ m/s, while keeping ten atomic planes at the bottom of the lower crystal fixed in the x direction. This gives an applied strain rate of approximately 2×10^7 s^{-1}. In this work, we focus on understanding the effect of different step geometries. No normal load is applied, and the contact interaction between the surfaces is purely by atomic interactions. To this end, atoms are unconstrained in the z direction, unless otherwise specified.

For a single step, the problem is not symmetric, and both loading directions are studied, indicated by step up and step down as shown in Fig. 2. For a step pair, the geometry is symmetric, therefore only loading in the positive x direction is studied.

An NPT ensemble is applied to mimic the material response at the nanoscale at room temperature, i.e., 300 K. The simulations in this work are performed with a thermostat applied to the whole system, with the intention of compensating for the inability of the model to capture heat conduction by the free electrons (similarly to the approach adopted by Gumbsch *et al.* [26] for a similar friction problem). However, we have also repeated our simulations with the thermostat applied only to the top and bottom regions and even without a thermostat. The results are negligibly affected, and no local melting or other significant unexpected local structure change occurred. Our conclusion is therefore that heat conduction is not greatly important for the studied problem.

III. CONTACTS WITH PERIODIC STEPS

A. Self-organized criticality of atomic scale friction

In this work, we start from perfect, dislocation-free crystals. We study the effect of a periodic array of single steps of small height, $\delta_0 = a/2$ and $\delta_0 = a$, on the friction behavior of a

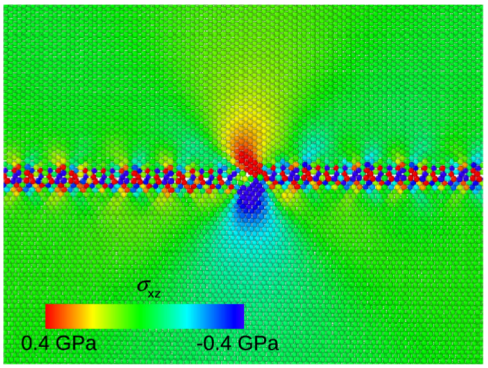

FIG. 3. Shear stress σ_{xz} in the vicinity of a single step (height $\delta = 0.405$ nm).

contact for both loading directions and compare the results with an atomically flat contact. The small step height results always in a closed contact. Figure 3 shows the σ_{xz} shear stress for step height $\delta_0 = a = 0.405$ nm. The stress concentration at the step arises due to closure of the contact. The system has been cooled to 1 K to visualize the stress.

The applied displacement first results in elastic shearing ($u_x < 2$ nm), as seen in Fig. 4, where results for various step spacings are shown, together with the response of a flat contact. The shear stress is defined as $\tau = F_x/(wd)$, where the total force F_x measured at the top of the upper crystal in the x direction is divided by the constant area wd. Contacts with different step density have the same elastic shearing response. The strength of the contact reaches about 500 MPa since the crystals do not contain initial dislocations.

At about $u_x = 2$ nm ($\gamma \approx 0.022$) sliding sets in resulting in a fluctuating friction stress ranging from about 400 to 900 MPa. In this work, "sliding" indicates the total displacement of one crystal with respect to the other, while "slip" indicates each discrete displacement jump occurring after a sticking period, as shown in Fig. 4. Decreasing the step spacing results in increased fluctuations in the friction stress, while the average

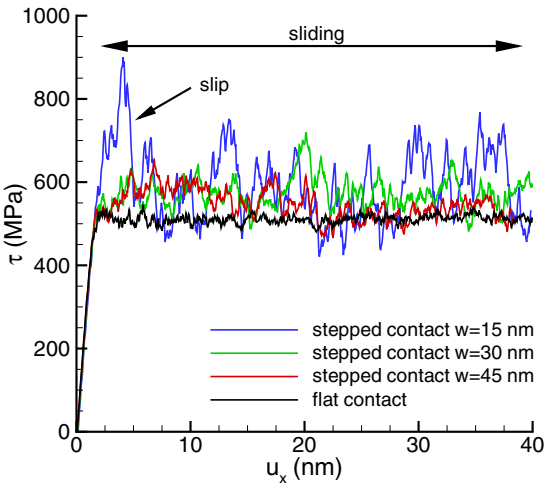

FIG. 4. Shear stress τ as a function of applied displacement u_x for different step spacing and for a flat contact, with the definition of sliding and slip depicted.

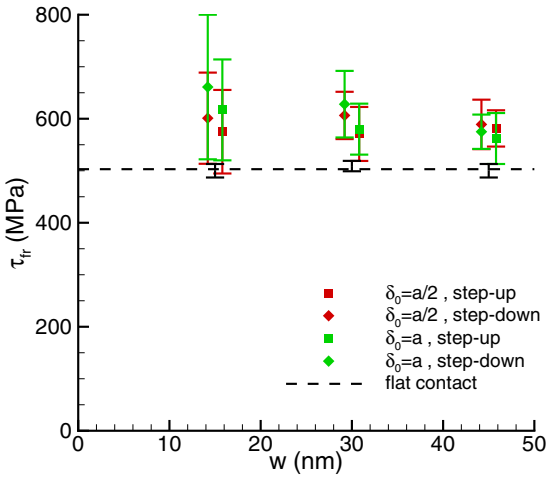

FIG. 5. Average and rms variation of friction stress τ_{fr} during sliding as a function of step spacing w for both sliding directions. For clarity the data points have been shifted by 0.8 nm.

friction stress increases only moderately. Every simulation is repeated four times with different initial atomic velocities (different realizations), to find the average behavior. The average friction stress τ_{fr} and the root mean square fluctuation are determined from the shear stress curves of the different realizations during sliding and shown in Fig. 5, for both loading directions.

The average friction stress τ_{fr} of stepped contacts is slightly higher than for a flat contact. More pronounced are the differences in terms of rms fluctuations of the friction stress. The difference is more pronounced for smaller step spacing, i.e., for rougher surfaces; while there are no visible differences in the loading direction.

The most important features of self-organized criticality are [27,28] (1) an abundance of metastable states, (2) the energy continuously put into the system is partly released in recognizable relaxation events, (3) the system is slowly driven away from the ground state so that the average waiting time between events and the event duration time are clearly separated, (4) the size of the relaxation events follows a power law distribution, and (5) all statistical properties should be stationary in the large-time limit, indicating that the attractor of the self-organized state is found. The subject of this work also includes these features: (1) the contact involves a large ensemble of atoms that during sliding are in meta-stable states, (2) the energy put into the system during 'stick' is released in recognizable relaxation events during "slip," i.e., there are stress drops in the friction stress, (3) in Fig. 4 it is clearly seen that the event duration time (slip) is much faster than the waiting time between events and hence the system is driven slowly, (4) the size of the stress drops S is given by power-law statistics $f(S) \propto S^{\beta}$ as shown in Fig. 6, (5) sliding occurs in the attractor state, which means that the stress drop statistics do not change over time. The attractor associated with the self-organized critical state depends on the step density. Therefore also the stress drop statistics are different for stepped or flat surfaces in contact (Fig. 6). For flat contacts, stress drops of smaller magnitude occur more often than for stepped contacts. For stepped contacts, stress drops

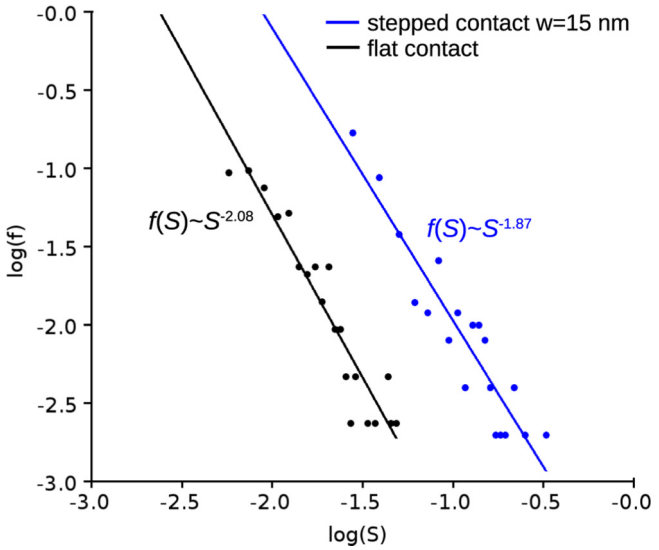

FIG. 6. Distribution $f(S)$ of the stress drops $S = \Delta\tau_d/\bar{\tau}$, where $\Delta\tau_d$ is the size of the stress drop and $\bar{\tau}$ is the average friction stress during sliding. The two limiting cases of Fig. 4 are shown, the stepped contact with spacing $w = 15$ nm and a flat contact. The intermediate cases $w = 30$ nm and $w = 45$ nm are between the two limits.

with larger magnitude are more frequent. Hence the power-law exponent for a stepped contact is $\beta_{\text{stepped}} = -1.87$ larger than for a flat contact $\beta_{\text{stepped}} = -2.08$, i.e., the stress that can build up and is released is larger for smaller step spacing (larger step density). The atomistic mechanisms that govern the stress drop-statistics for stepped contacts are various: not only local slip across the step, but also step motion and contact migration, as will be discussed in the following section.

B. Normal contact migration

A closer look at the sliding process of the stepped contacts reveals that additional to slip at the contact, another mechanisms occurs: motion of the step along the contact resulting in normal migration of the entire contact. Migration of the contact is a stress relaxation mechanism that competes with contact slip.

The direction of migration depends on the loading direction as shown in Fig. 7. The contact migration is a consequence of the motion of the step similar to the mechanism for grain boundary migration discussed in Refs. [29–31]. In Refs. [29,30], it is explained how local atomic rearrangement leads to step motion from which the migration results. In Ref. [31], it is found that grain boundaries that are intrinsically immobile become mobile through additional line-defects like steps. The phenomenon is analogous to re-crystallization (see Fig. 7). A unit displacement of the step in the horizontal direction induces a unit displacement in the vertical direction. Inverting the loading direction inverts the stress state and hence results in step motion and contact migration in the opposite direction.

Figure 8 shows the absolute normal migration distance $|u_n|$ per unit applied displacement as a function of step spacing. As to be expected with increasing step density, the normal migration increases.

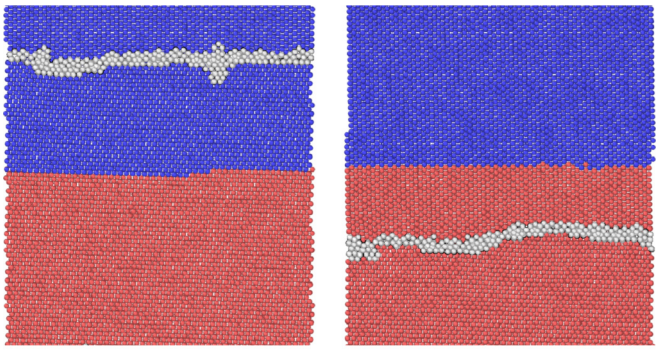

FIG. 7. Contact migration at $u_x = 40$ nm for (a) the step-up loading direction and (b) the step-down loading direction. Atoms that originally belong to crystal A (B) are indicated with the color red (blue). The grey atoms indicate the new position of the contact, based on CNA.

Figure 8 shows that for $\delta_0 = a/2$ in the step-down direction, the migration distance is significantly lower than in the other cases, and thus contact slip prevails over contact migration since during sliding the total sliding displacement equals the applied displacement. The cause for the prevailing local slip across the step in the step-down loading direction is due to the asymmetry of the Ehrlich-Schwoebel barrier [10,11] as shown in Fig. 9. For slipping across the step in the step-up direction, atoms have to come out of a low energy well and be pushed over a high energy barrier. For slipping across the step in the step-down direction, atoms have to cross a lower energy barrier towards a lower energy level and hence slipping across the step is facilitated. With increasing step height, also the barrier height increases and hence only when the step height is large enough ($\delta_0 = a$), the barrier height becomes so large that slipping across the step is unfavorable so that for both sliding directions step motion is promoted.

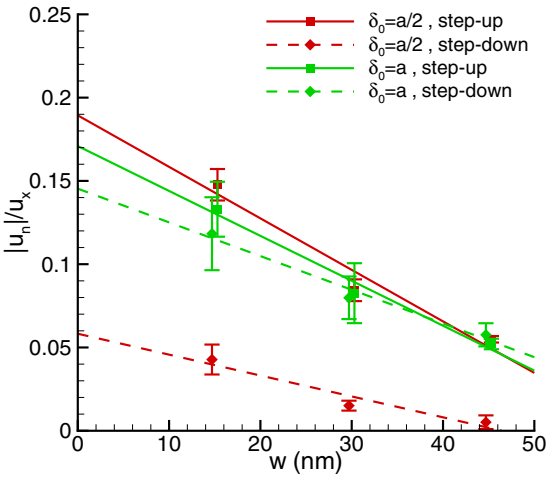

FIG. 8. Normal migration distance $|u_n|$ per unit applied displacement as a function of step spacing (i.e., box width). For clarity, the data points have been shifted ± 0.3 nm for the positive and negative x direction, respectively. The error bars denote the rms variation in the normal migration.

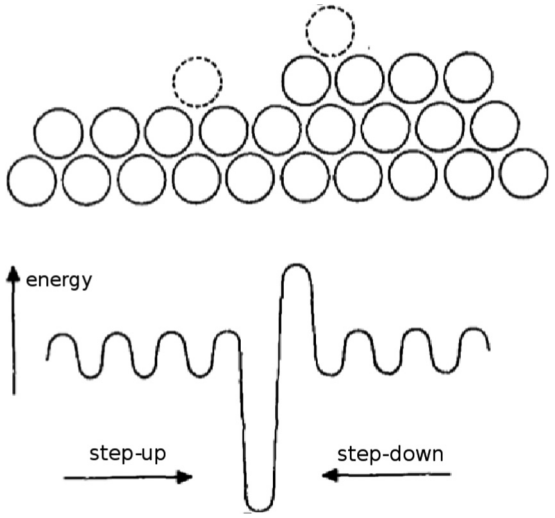

FIG. 9. Ehrlich-Schwoebel barrier [10,11] showing the asymmetry of the potential landscape near the step.

Interestingly, for steps of height $a_0/2$ slip over the step and step motion involve energy barriers that have similar height, so that the friction stress is independent of loading direction (see Fig. 5), although in one direction local slip across the step dominates over step motion and in the other direction step motion dominates over local slip across the step.

Rare migration reversal

In most cases normal migration occurs in one particular direction, related to the loading direction. However, there are cases where the direction of migration is reversed, as can be seen in Fig. 10 where the average z coordinate of the contact is presented. Reversal occurs at about $u_x = 10$ nm. This is caused by the nucleation of dislocations, which cause a change in the sign of the step. In an fcc metal, it is often energetically favorable for a dislocation to split into two partial dislocations separated by a stacking fault, and this is also the case for Al. The atoms in the stacking fault ribbon have a local HCP

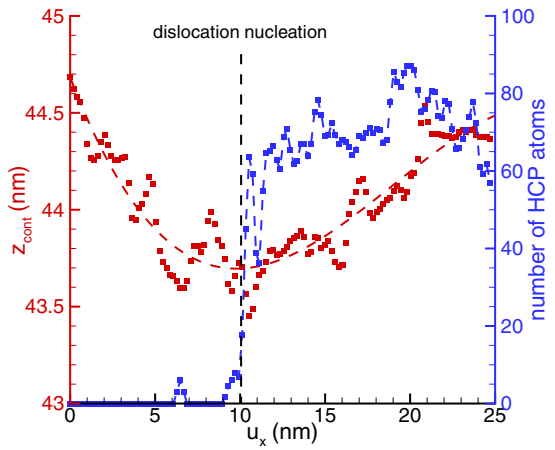

FIG. 10. Average z coordinate of the contact (red) and the number of atoms with HCP structure (blue) as a function of applied displacement.

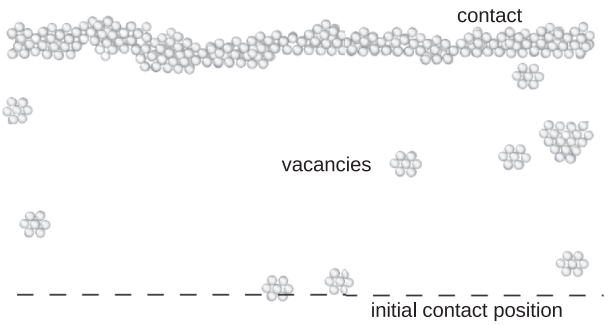

FIG. 11. Contact after 40 nm applied displacement in the positive x direction, clearly showing vacancies generated between the initial and the current position of the contact. Only atoms that do not have a perfect local fcc structure are shown.

structure, so that the number of atoms with HCP structure is a measure of the number of dislocations in the material.

In Fig. 10, it is shown that initially there are no atoms with HCP structure in the system (based on a common neighbor analysis, CNA [32], excluding the contact), i.e., there are no dislocations. Only at an applied displacement of about 10 nm, significantly beyond the onset of sliding as seen in Fig. 4, dislocation nucleation occurs. The number of HCP atoms, on average approximately 65, and the separation of the partials, indicates that two dislocations (four partial dislocations) are nucleated. It is the nucleation of these two dislocations that changes the sign of the step in the contact and causes the reversal of the migration direction. Migration reversal by dislocation nucleation is a rare event in simulations with a negligible normal loading, as it was only found in 1 out of 24 cases studied.

C. Vacancy generation

A contact, flat or stepped, between two crystals with different orientation entails a certain excess free volume compared with the perfect crystal, so that the contact can be thought of as a potential reservoir of vacancies. It has been reported that curvature driven grain boundary migration can result in the generation of vacancies to accommodate the excess free volume [33] associated with the decrease in the grain boundary volume. For a flat contact in this study, it has been found that upon applied tangential displacement, pure slip at the contact occurs, and the excess free volume at the contact is unchanged. However, as just shown, a stepped contact migrates in the normal direction, which is similar to a recrystallization process. It is found that this re-crystallization can result in the generation of vacancies, which are found in the re-crystallized part of the bicrystal [34]. This is shown in Fig. 11, where only atoms that do not have a perfect local fcc structure are represented.

It is important to realize that this vacancy generation is found to take place at room temperature. The local vacancy concentration near the contact that results from the normal migration is more than two orders of magnitude higher than the equilibrium vacancy concentration at room temperature. We expect that in cases when both plastic deformation and contact migration occur together, dislocation climb might even occur

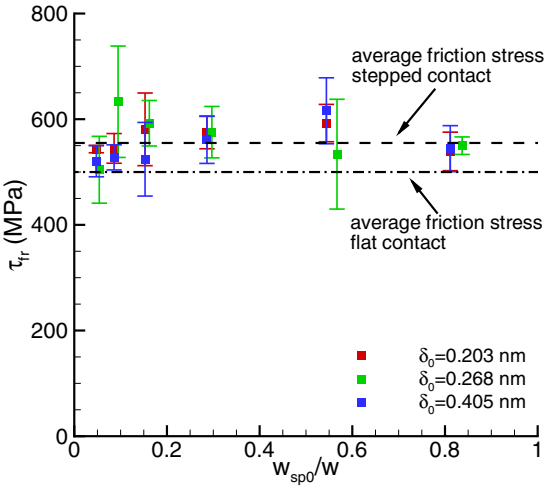

FIG. 12. Average and rms variation of the friction stress as a function of normalized pair spacing w_{sp0}/w for several step heights. The line for the flat contact is the same as in Fig. 4.

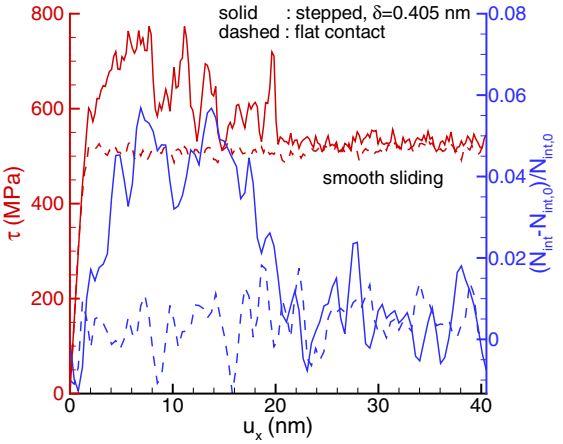

FIG. 13. Example of shear stress τ (red) and fractional interface roughness $(N_{int} - N_{int,0})/N_{int,0}$ (blue) as function of applied displacement u_x. A comparison of the two graphs shows that the large fluctuations in the friction stress coincide with the roughened contact.

at room temperature. Experimental observations of dislocation climb in Al/Nb multilayers indicates that dislocation climb can indeed occur at room temperature due to high vacancy concentration in the interfaces [35].

IV. CONTACTS WITH PERIODIC STEP PAIRS

A. Small step height

In this section, we will study the friction behavior of step pairs and compare it to that of periodic single steps and atomically flat contacts. The step pairs introduce an additional parameter, the width between the opposite steps w_{sp0}. To study the effect of w_{sp0}, we choose one specific box width $w = 30$ nm and vary the pair width. For each case four simulations with different initial atomic velocities are performed. Figure 12 shows the average friction stress and its rms variation during sliding as a function of the step pair width to spacing ratio, w_{sp0}/w, for three different step heights and for the flat contact. We find that the average friction stress is not significantly affected by the width of the step pair. This might seem surprising at first sight, but the absence of a clear trend is due to the fact that the steps move independently in a stochastic manner, so that the initial configuration is soon lost during sliding.

In the previous section, it was shown that a self-organized critical state is involved in sliding friction and that the fluctuations in the friction stress are larger at smaller step spacing. Interestingly, for the periodic step pair contacts it is found that there exist two sliding states: one being "jerky" with large stress fluctuations, the second one being "smooth" with small fluctuations (Fig. 13). The smooth sliding state is associated with the attractor: sliding can transit through self-organization from the jerky state into the smooth state. This self-organization is carried by the atomic rearrangement of the contact. Figure 13 shows an example for which the transition between jerky sliding and smooth sliding occurs at about $u_x = 20$ nm. Also the fractional change in the number of interface atoms (non-fcc atoms) N_{int}, $(N_{int} - N_{int,0})/N_{int,0}$, as a measure of the interface roughness is shown. It is seen that the decrease in interface roughness coincides with the jerky-smooth sliding transition. From start the steps are separated, and hence the contact has a jagged roughness. The components of the steps are observed to move individually, thereby initially maintaining the jagged roughness [Fig. 14(a)]. Although the steps are opposite, they do not annihilate, since there is still an excess volume with respect to a flat contact. In the process of sliding, atomic rearrangement (self-organization) through step motion results in an evolving contact topology, i.e., lower roughness. Eventually, the self-organization results in a flatter contact, since the constituents of the step pair organize in a low-energy configuration, which results in a "wave" that travels through the contact during sliding opposite to the loading direction, as shown in Fig. 14(b) [37].

Recently, a combined computational and experimental study of wear of metal surfaces scratched with a tip pointed towards an analogy with laminar and turbulent flow [26,36]. However, in Refs. [26,36], laminar plastic flow developed into turbulent plastic flow. The transition found in the present work is from a "turbulent" state into a "laminar" state. Processes at the atomic scale control energy dissipation at the nanometer or even micrometer scale. Obviously, the stress drop statistics are significantly different in the jerky state compared to the smooth

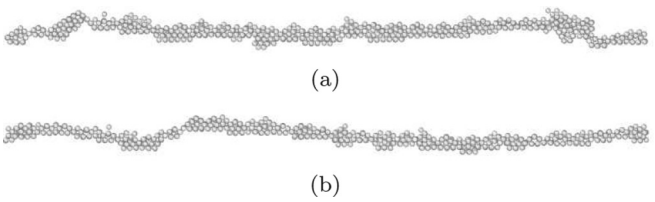

FIG. 14. The contact structure showing (a) jagged roughness in the jerky sliding stage at $u_x \approx 8$ nm and (b) a smooth "wave" in the contact during the smooth sliding stage at $u_x \approx 30$ nm. Atoms that do not belong to the interface, i.e., that have fcc structure type, are excluded.

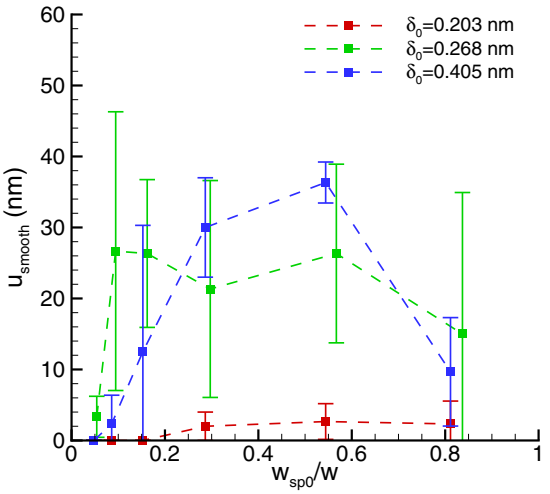

FIG. 15. Average sliding displacement and rms variation (between different realizations) at which the transition to smooth sliding occurs as a function of the relative pair width.

sliding state. The jerky state is similar to sliding friction of a contact with large step density, while the smooth sliding state is similar to sliding of a flat contact.

The sliding displacement u_{smooth} at which the transition to smooth sliding occurs, defined as the displacement between the onset of sliding and the transition, is shown in Fig. 15 as a function of w_{sp0}/w. For the smallest step height, the transition is almost immediate once sliding is initiated. For larger step height, significant atomic rearrangement is involved (Fig. 14) and the transition is found to take place at greatly varying displacements for different initial conditions (realizations).

One final note on the possibility of contact migration of step pair surfaces in contact. Because the steps are initially opposite, there is no net migration, since one of the steps causes migration upwards, while the other causes migration downwards, effectively canceling each other. However, as found in the previous section, dislocation nucleation from the contact can statistically occur. This leads to a net step height in the contact, which undoes the cancellation, and therefore leads to migration of the contact. Since this is found to occur in only about 10% of the cases, without correlation with pair spacing or step height, we consider it of only minor significance in the friction behavior of stepped surfaces in spite of its fundamental interest.

A note on shearing with a normal load applied

The simulations of the step pair contacts, were repeated after applying a normal load to the contact, to highlight the effect of dislocation nucleation. With the application of normal load it is indeed expected that dislocation and twin nucleation from the steps becomes relevant. It is found that up to an applied normal load of 3 GPa no dislocation and/or nucleation during normal loading occurs. However, as shearing sets in, the higher the normal load, the more likely the nucleation of dislocations and/or twins becomes. Above a normal load of 1.5 GPa, we always observe dislocation and/or twin nucleation. When dislocation/twin nucleation occurs the transition between jerky and smooth sliding is no longer

FIG. 16. Contact with nanoscale asperities for case AB. Atoms that do not belong to the interface, i.e., that have fcc structure type, are excluded.

observed. This is because the nucleation of a dislocation/twin affects the net step height of the contact which from zero becomes b. The presence of a net step height leads to contact migration and smooth sliding is never achieved. Below a normal load of 1.5 GPa, the likelihood of observing jerky-smooth sliding transition decreases with increasing normal load.

B. Large step height: nanoscale asperities

In this section, we will study the friction behavior of contacts with step pairs of large height, $\delta \approx 1.5$ nm. After relaxation the contact does not close, resulting in a gap. The contact can be thought of as being made by a surface consisting of a periodic array of nanoscale asperities of various widths w_{sp0} touching an atomically flat surface. The normalized contact area is then given by

$$\frac{A_{\text{r}}}{wd} = \frac{w - w_{\text{sp}}}{w}. \tag{1}$$

Here, A_{r} is the contact area, d is the periodicity in the small y direction. The contact area is not always constant during shearing, therefore for characterization we will use A_{r0}, w_{sp0} and δ_0 for the initial contact area, step pair width and step height, respectively. Without subscript $_0$, the variables refer to evolving quantities.

Figure 16 shows an example of the initial contact structure with a clear gap. Two cases are studied: case AB, crystal A has a stepped surface and crystal B a flat surface, and case BA, for which the situation is reversed.

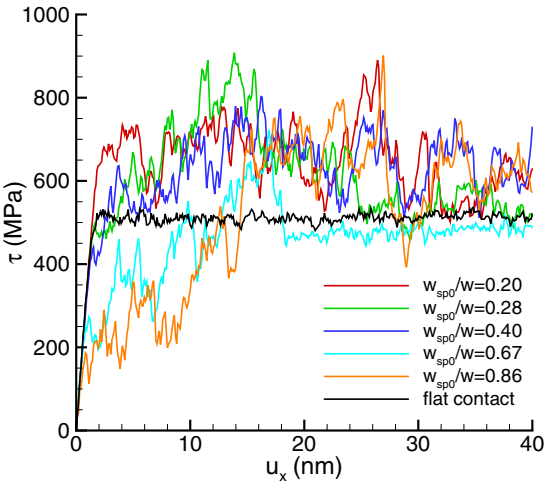

FIG. 17. Shear stress as a function of applied displacement for different step pair widths (for large step height). One curve (light blue) shows the statistical transition to smooth sliding similar to the transition found for small height step pairs.

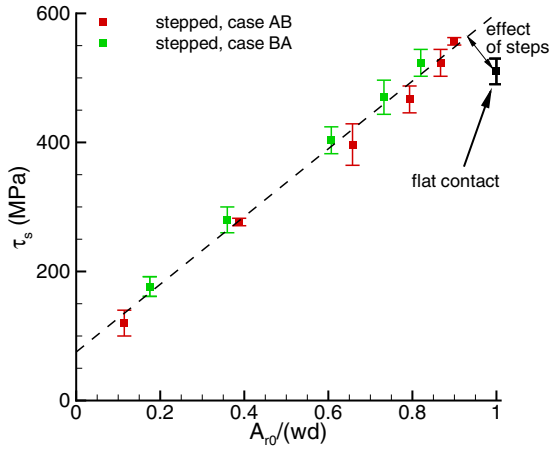

FIG. 18. Static friction stress as a function of the normalized contact area. Error bars give the rms variation between different realizations.

Figure 17 shows the shear stress as a function of applied displacement for different w_{sp0}/w. Larger w_{sp0}/w entails smaller initial contact area leading to larger contact stress and hence an earlier onset of sliding as seen in Fig. 17. Figure 18 shows the static friction stress τ_s (taken at 1 nm offset displacement) as a function of the normalized initial contact area $A_{r0}/(wd)$ for the two different cases. Both cases show a linear relation in τ_s with contact area. Stepped surfaces give clearly a larger static friction stress than a flat contact.

In Fig. 19, it can be seen that during sliding, material is transferred from one surface to the other. In Ref. [39] it is observed that surface roughness is essential for wear to occur. This observation is also made in the present work: atomically flat contacts slide with respect to each other, and wear (local material transfer from one crystal to the other) only occurs when there is roughness in the form of steps. This is similar to the re-crystallization process observed previously for single periodic steps, except for the fact that here the contact topology changes drastically by material transfer, and hence it is appropriate to refer to it as a wear process [38]. The other difference is that the contact does not migrate, unless dislocation nucleation occurs, and therefore the vacancies that

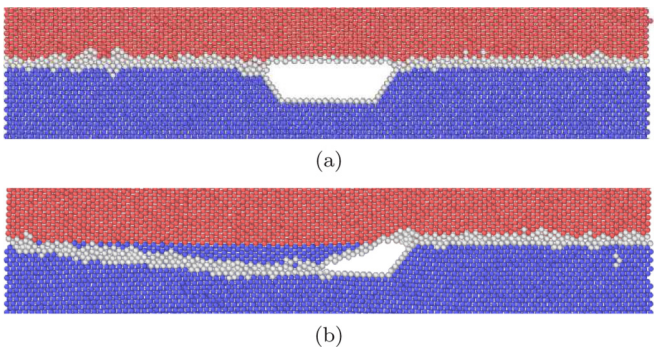

FIG. 19. (a) The initial contact (case AB), atoms that originally belong to crystal A(B) are indicated with the color blue(red). The grey atoms indicate the position of the contact, based on CNA. (b) Developing wear at $u_x \approx 5$ nm.

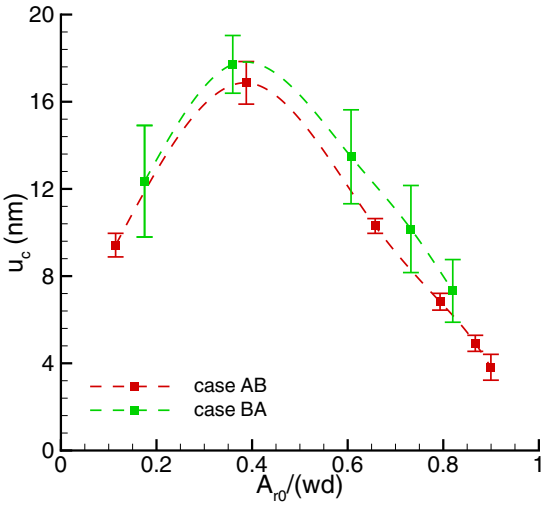

FIG. 20. Sliding displacement to closure u_c as a function of normalized contact area. This is the difference in applied displacement between the onset of sliding and full closure of the gap. The error bars indicate the rms variation between different realizations.

are generated are re-absorbed during sliding. Due to atomic wear the contact area increases, i.e., the gap decreases, until full contact is reached. This increase in contact area is the cause for the increase in τ at small shearing displacement in Fig. 17.

Figure 20 shows the sliding displacement u_c needed for the gap to completely close. For large step pair width, i.e., small contact area, lesser material of the small asperity is available to be transferred until full contact is reached, and therefore the gap closes at rather low sliding displacement. At small step pair width, i.e., large contact area, only a small amount of material is needed to be transferred from one surface to the other to close the gap, so that also in this case the gap closes at rather low sliding displacement. At intermediate step pair width, the sliding displacement to closure is larger. The maximum does not occur at $A_{r0}/(wd) = 0.5$, since the closure is a nonlinear process in which the interaction between the free surfaces is involved, leading to sudden gap closure when the distance between the free surfaces becomes small enough. The wear process is especially important when the initial contact area is small, when the largest difference is found between the static friction stress and the sliding friction stress in the large u_x limit.

As the gap closes, the free surface area decreases, together with the potential energy (change in the order of 1 meV/atom). The dissipated energy in this process is in reality absorbed by a large heat bath. Since our simulations consider a rather limited systems size, the thermostat takes care of the absorption of the generated heat. Once the gap is completely closed, the friction stress is statistically independent of w_{sp0}/w, i.e., the behavior becomes like the behavior of step pair contacts with small contact height, as discussed in the previous section.

V. CONCLUSIONS

Room-temperature molecular dynamics simulations of contact friction between two differently oriented Al crystals have

yielded the following results. (1) Sliding friction of stepped surfaces has all the properties of self-organized criticality. The power law slip statistics depend on the step spacing: large slip events are much more probable for contacts with small step spacing than for contacts in the large spacing limit, i.e., atomically flat contacts. (2) Apart from slipping, atomic steps can move along the contact, concurrently resulting in contact migration perpendicular to the contact plane. Contact migration occurs only when there is a net step height, it is a recrystallization phenomenon and results in vacancy generation near the contact. (3) When the steps are in pairs, there is no net step height and overall migration of the contact does not take place. The stick-slip behavior of these contacts occurs in two clearly distinguishable stages, first jerky with large stick and slip events, then smooth and similar to a flat surface. The two stages are separated by a marked transition. The friction behavior is statistically independent of step pair width. (4) Step pair contacts of large height, where there is a gap between the surface, suffer from wear, which results in a growing contact area, eventually making the friction behavior similar to that of small height step pair contacts.

ACKNOWLEDGMENTS

This work is part of the research programme of the Foundation for Fundamental Research on Matter (FOM), which is part of the Netherlands Organisation for Scientific Research (NWO).

[1] E. Vlieg, A. W. Denier van der Gon, J. F. van der Veen, J. E. Macdonald, and C. Norris, Surface X-Ray Scattering During Crystal Growth: Ge on Ge(111), Phys. Rev. Lett. **61**, 2241 (1988).

[2] J. F. Lutsko, A. E. S. Van Driessche, M. A. Durán-Olivencia, D. Maes, and M. Sleutel, Step Crowding Effects Dampen the Stochasticity of Crystal Growth Kinetics, Phys. Rev. Lett. **116**, 015501 (2016).

[3] R. J. Dikken, B. J. Thijsse, and L. Nicola, Impingement of edge dislocations on atomically rough contacts, Comput. Mater. Sci. **128**, 310 (2017).

[4] T. Shimokawa, T. Kinari, and S. Shintaku, Interaction mechanism between edge dislocations and asymmetrical tilt grain boundaries investigated via quasicontinuum simulations, Phys. Rev. B **75**, 144108 (2007).

[5] S. H. Oh, M. Legros, D. Kiener, and G. Dehm, In situ observation of dislocation nucleation and escape in a submicrometre aluminium single crystal, Nat. Mater. **8**, 95 (2009).

[6] B. Luan and M. O. Robbins, The breakdown of continuum models for mechanical contacts, Nature (London) **435**, 929 (2005).

[7] T. Müller, M. Lohrmann, T. Kässer, O. Marti, J. Mlynek, and G. Krausch, Frictional Force between a Sharp Asperity and a Surface Step, Phys. Rev. Lett. **79**, 5066 (1997).

[8] K. Meine, T. Schneider, D. Spaltmann, and E. Santner, The influence of roughness on friction, Part I: The influence of a single step, Wear **253**, 725 (2002).

[9] H. Hölscher, D. Ebeling, and U. D. Schwarz, Friction at Atomic-Scale Surface Steps: Experiment and Theory, Phys. Rev. Lett. **101**, 246105 (2008).

[10] G. Ehrlich and F. G. Hudda, Atomic view of surface self-diffusion: tungsten on tungsten, J. Chem. Phys. **44**, 1039 (1965).

[11] R. L. Schwoebel and E. J. Shipsey, Step motion on crystal surfaces, J. Appl. Phys. **37**, 3682 (1966).

[12] N. Abdolrahim, I. N. Mastorakos, S. Shao, D. F. Bahr, and H. M. Zbib, The effect of interfacial imperfections on plastic deformation in nanoscale metallic multilayer composites, Comput. Mater. Sci. **86**, 118 (2014).

[13] J. B. Sokoloff, Possible microscopic explanation of the virtually universal occurrence of static friction, Phys. Rev. B **65**, 115415 (2002).

[14] N. Q. Vo, R. S. Averback, P. Bellon, S. Odunuga, and A. Caro, Quantitative description of plastic deformation in nanocrystalline Cu: Dislocation glide versus grain boundary sliding, Phys. Rev. B **77**, 134108 (2008).

[15] P. Bak, C. Tang, and K. Wiesenfeld, Self-Organized Criticality: An Explanation of 1/f Noise, Phys. Rev. Lett. **59**, 381 (1987).

[16] P. Bak, C. Tang, and K. Wiesenfeld, Self-organized criticality, Phys. Rev. A **38**, 364 (1988).

[17] H. J. Feder and J. Feder, Self-Organized Criticality in a Stick-Slip Process, Phys. Rev. Lett. **66**, 2669 (1991).

[18] F. R. Zypman, J. Ferrante, M. Jansen, K. Scanlon, and P. Abel, Evidence of self-organized criticality in dry sliding friction, J. Phys.: Condens. Matter **15**, L191 (2003).

[19] S. V. Buldyrev, J. Ferrante, and F. R. Zypman, Dry friction avalanches: Experiment and theory, Phys. Rev. E **74**, 066110 (2006).

[20] P. Creeger and F. Zypman, Entropy content during nanometric stick-slip motion, Entropy **16**, 3062 (2014).

[21] S. J. Plimpton, Fast parallel algorithms for short-range molecular dynamics, J. Comput. Phys. **117**, 1 (1995).

[22] M. S. Daw, M. I. Baskes, Embedded-atom method: Derivation and application to impurities, surfaces and other defects in metals, Phys. Rev. B **29**, 6443 (1984).

[23] G. P. Purja Pun and Y. Mishin, Development of an interatomic potential for the Ni-Al system, Philos. Mag. **89**, 3245 (2009).

[24] Y. Mishin, D. Farkas, M. J. Mehl, and D. A. Papaconstantopoulos, Interatomic potentials for monoatomic metals from experimental data and ab initio calculations, Phys. Rev. B **59**, 3393 (1999).

[25] Y. Mishin, Atomistic modeling of the γ and γ'-phases of the NiAl system, Acta Mater. **52**, 1451 (2004).

[26] N. Beckmann, P. A. Romero, D. Linsler, M. Dienwiebel, U. Stolz, M. Moseler, and P. Gumbsch, Origins of Folding Instabilities on Polycrystalline Metal Surfaces, Phys. Rev. Appl. **2**, 064004 (2014).

[27] B. Persson and E. Tosatti, *Physics of Sliding Friction* (Kluwer, Dordrecht, 1996).

[28] M. Nosonovsky and B. Bhushan, *Multiscale Dissipative Mechanisms and Hierarchical Surfaces: Friction, Superhydrophobicity, and Biomimetics* (Springer, Heidelberg, 2008).

[29] A. Rajabzadeh, F. Mompiou, M. Legros, and N. Combe, Elementary Mechanisms of Shear-Coupled Grain Boundary Migration, Phys. Rev. Lett. **110**, 265507 (2013).

[30] N. Combe, F. Mompiou, and M. Legros, Disconnections kinks and competing modes in shear-coupled grain boundary migration, Phys. Rev. B **93**, 024109 (2016).

[31] C. P. Race, R. Hadian, J. von Pezold, B. Grabowski, and J. Neugebauer, Mechanisms and kinetics of the migration of grain boundaries containing extended defects, Phys. Rev. B **92**, 174115 (2015).

[32] A. Stukowski, Structure identification methods for atomistic simulations of crystalline materials, Modelling Simul. Mater. Sci. Eng. **20**, 045021 (2012).

[33] M. Upmanyu, D. J. Srolovitz, L. S. Shvindlerman, and G. Gottstein, Vacancy generation during grain boundary migration, Int. Sci. **6**, 287 (1998).

[34] See Supplemental Material at http://link.aps.org/supplemental/10.1103/PhysRevB.95.104106 for a movie of contact migration resulting in vacancy generation.

[35] N. Li, J. Wang, J. Y. Huang, A. Misra, and X. Zhang, In situ TEM observations of room temperature dislocation climb at interfaces in nanolayered Al/Nb composites, Scr. Mater. **63**(4), 363 (2010).

[36] N. K. Sundaram, Y. Guo, and S. Chandrasekar, Mesoscale Folding, Instability, and Disruption of Laminar Flow in Metal Surfaces, Phys. Rev. Lett. **109**, 106001 (2012).

[37] See Supplemental Material at http://link.aps.org/supplemental/10.1103/PhysRevB.95.104106 for a movie of the contact topology showing the transition from jerky to smooth sliding.

[38] T. D. B. Jacobs and R. W. Carpick, Nanoscale wear as a stress-assisted chemical reaction, Nat. Nanotechnol. **8**, 108 (2013).

[39] J. A. Harrison and D. W. Brenner, Simulated tribochemistry: an atomic-scale view of the wear of diamond, J. Am. Chem. Soc. **116**, 10399 (1994).